The 1st International Workshop on Physics at High Baryon Density (PHD2024)

Collision Energy Dependence of the Light- and Hyper-Nuclei Directed Flow in 3.0-4.5 GeV Au+Au Collisions at RHIC-STAR

Chengdong Han

Institute of Modern Physics, CAS
chdhan@impcas.ac.cn

2024/11/03

Outline

1. Introduction
2. Dataset and Particle Reconstruction
3. Light- and Hyper-Nuclei Collective Flow
    1. Light- and Hyper-Nuclei Directed Flow v_1
    2. Mass and Energy Dependence of v_1
4. Summary and Outlook

High-Energy Nuclear Collisions and QCD Phase Diagram

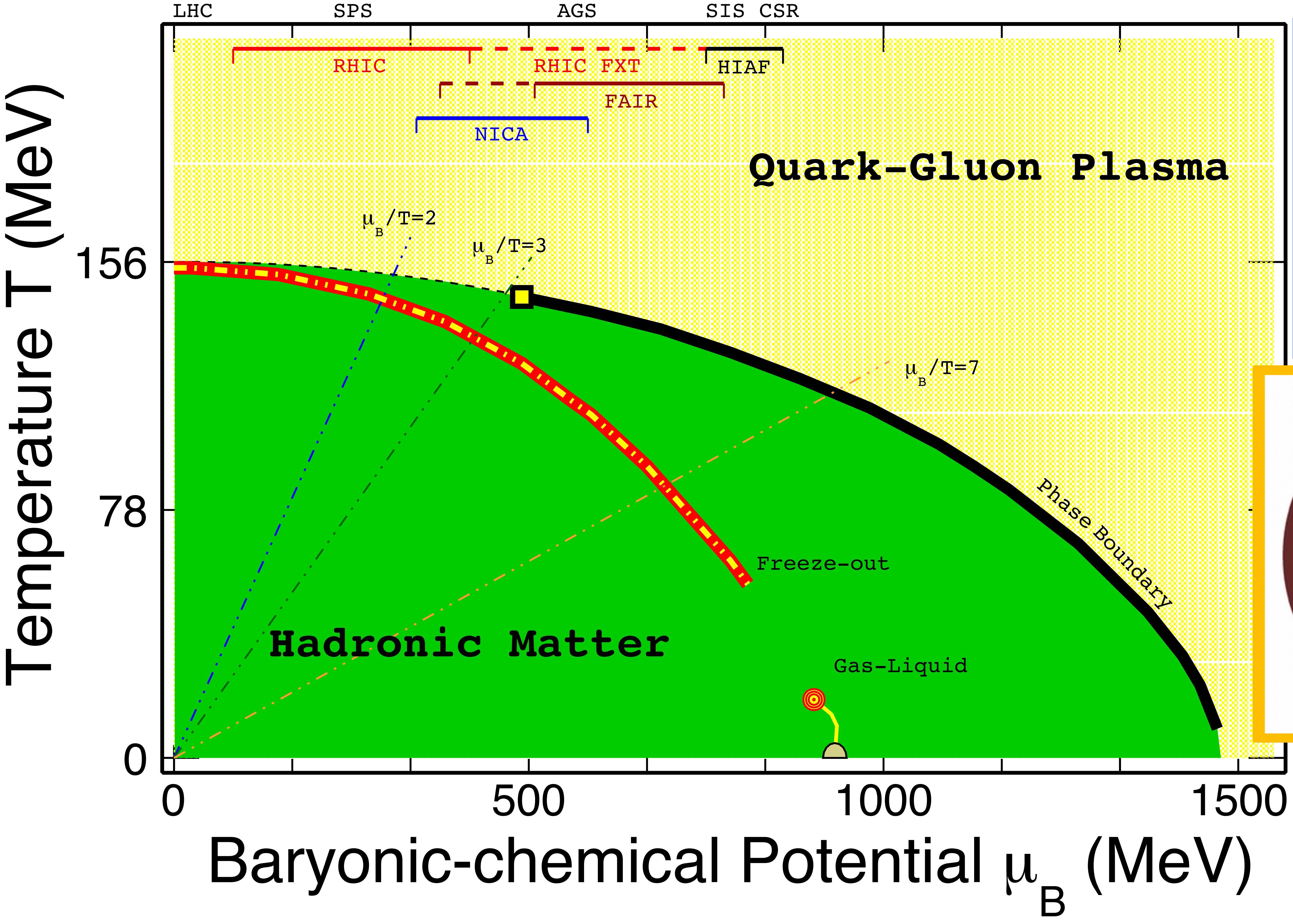

Hyperon Puzzle: difficulty to reconcile the measured masses of neutron stars with the presence of the hyperons in their interiors

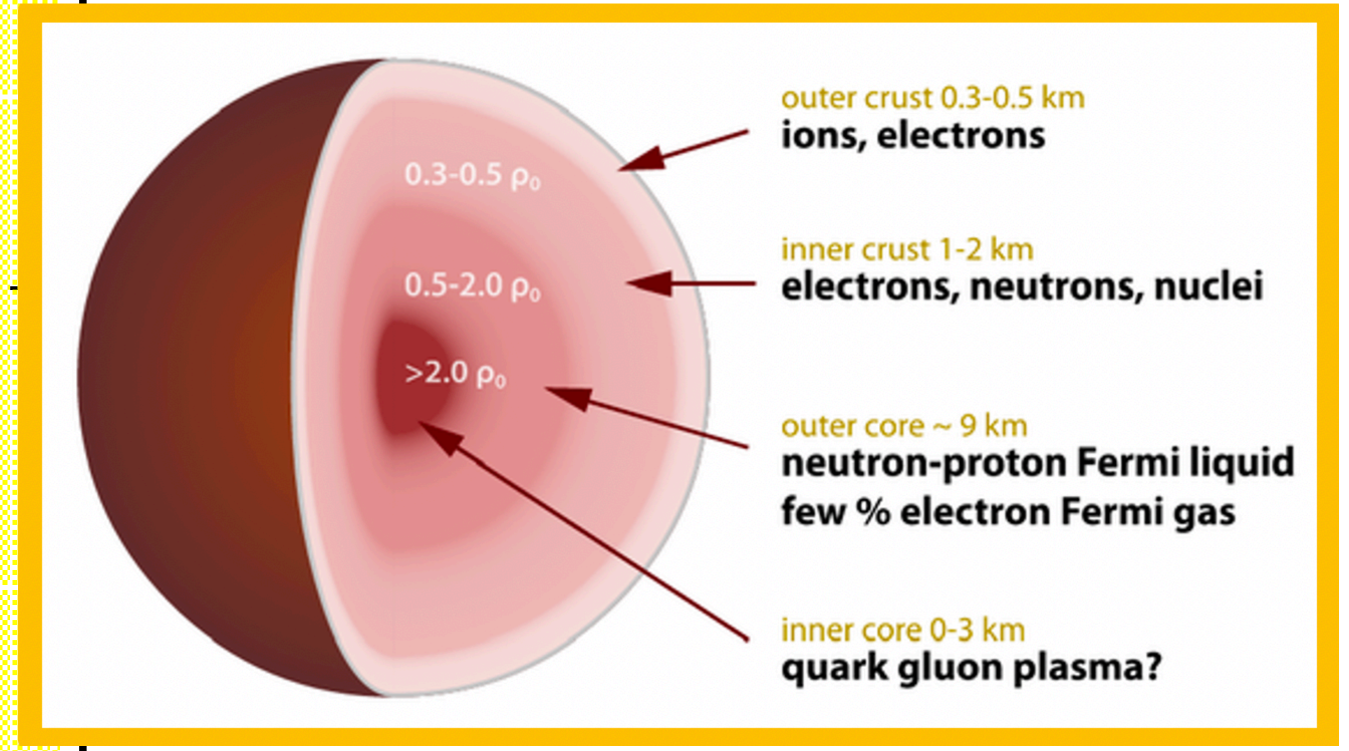

1) RHIC beam energy scan → search for 1st-order phase transition and QCD critical point
2) Baryon-baryon interaction (*e.g.* N-N, Y-N) → inner structure of compact stars

Light- and Hyper-nuclei Productions

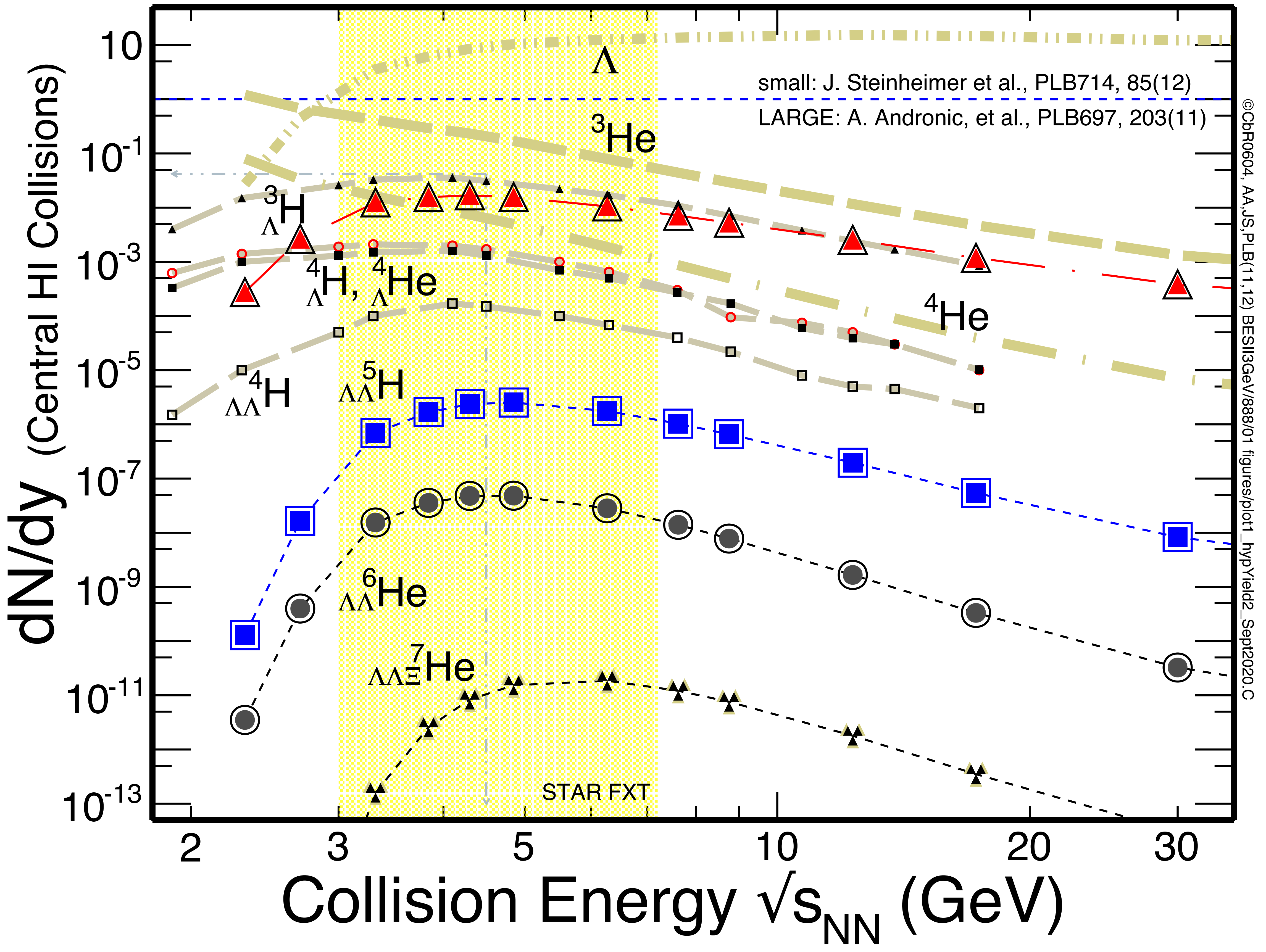

[1] A. Andronic *et al*. Phys.Lett.B 697, 203 (2011)
[2] J. Steinheimer *et al*. Phys.Lett.B 714, 85 (2012)

1) Light- and Hyper-Nuclei are abundantly produced at high baryon density region

2) Light-Nuclei carry information about local baryon density fluctuations at freeze-out; offers insights on the Final State Interaction: N-N

3) Hyper-Nuclei provide access to the hyperon–nucleon interaction: Y-N

4) Collective flow is sensitive to the Equation-of-State of nuclear matter

Collective Flow

Heavy ion collisions: Initial spatial anisotropy → Pressure gradient → Anisotropic flow

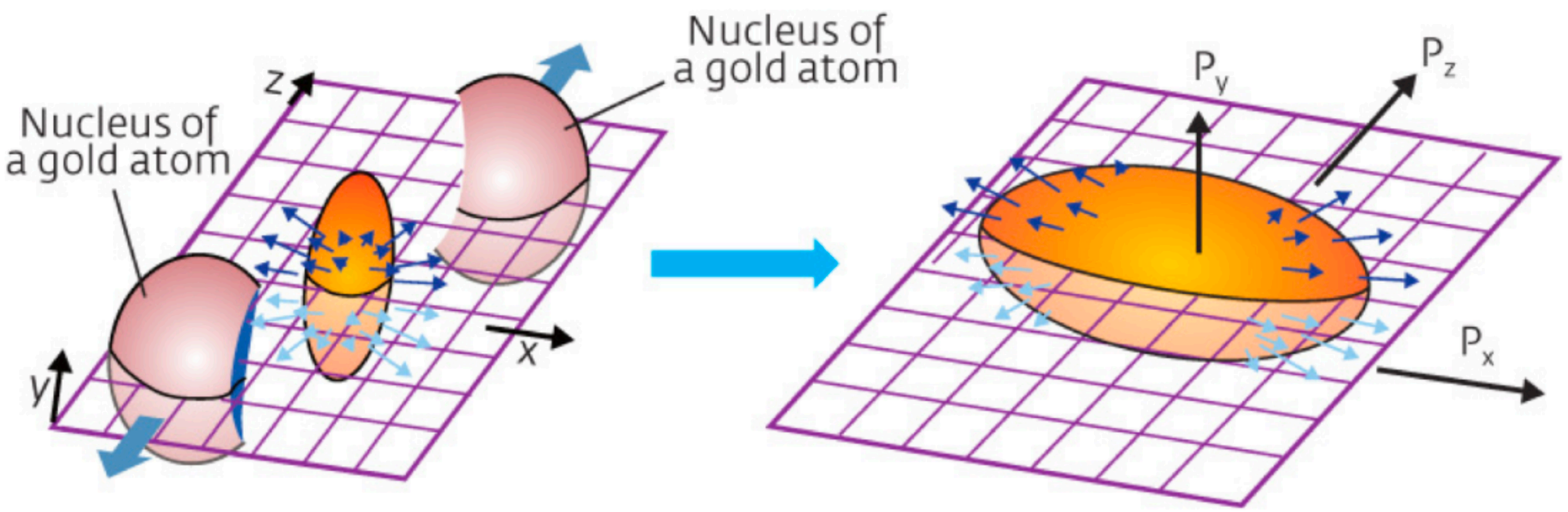

$$v_1 = < p_x/p_T > \qquad v_2 = < (p_x^2 - p_y^2)/p_T^2 >$$

1) The initial pressure gradient of the collision system is directly related to the magnitude of v_n, which is a sensitive observable for studying EoS
2) Collectivity of light- and hyper-nuclei in heavy-ion collisions at high baryon density regions is important for understanding their formation mechanism

Collective Flow analysis

- The n^th order coefficient of the fourier expansion of the azimuthal distribution in the momentum space

$$E\frac{d^3N}{dp^3} = \frac{1}{2\pi}\frac{d^2N}{p_T dp_T dy}\left(1+\sum_{1}^{\infty} 2v_n \cos\left[n\left(\phi-\psi_{RP}\right)\right]\right)$$

— v_1 ***Directed flow*** — v_2 ***Elliptic flow***

Analysis steps with event plane method

1) Signal extraction for a given ϕ - Ψ_n bin:

$$N^R(\phi-\psi_n) = \int dM \frac{1}{R_n}\frac{dN}{d(\phi-\psi_n)}$$

2) Fit dN/d(ϕ - Ψ_n) distribution in rapidity bins to extract observed flow coefficients v_n^R

3) Correct v_n^R with signal number weighted EP resolution $< \frac{1}{R_n} >$:

$$< v_n > = < v_n^R > < \frac{1}{R_n} >$$

$$< \frac{1}{R_n} > = \frac{\Sigma_i N_i * < \frac{1}{R_n} >}{\Sigma_i N_i}$$

[1] H. Masui *et al*., Nucl. Instrum. Methods Phys. Res. A **833**, 181 (2016)
[2] A. M. Poskanzer and S. A. Voloshin, Phys. Rev. C **58,** 1671 (1998)

STAR Detector System

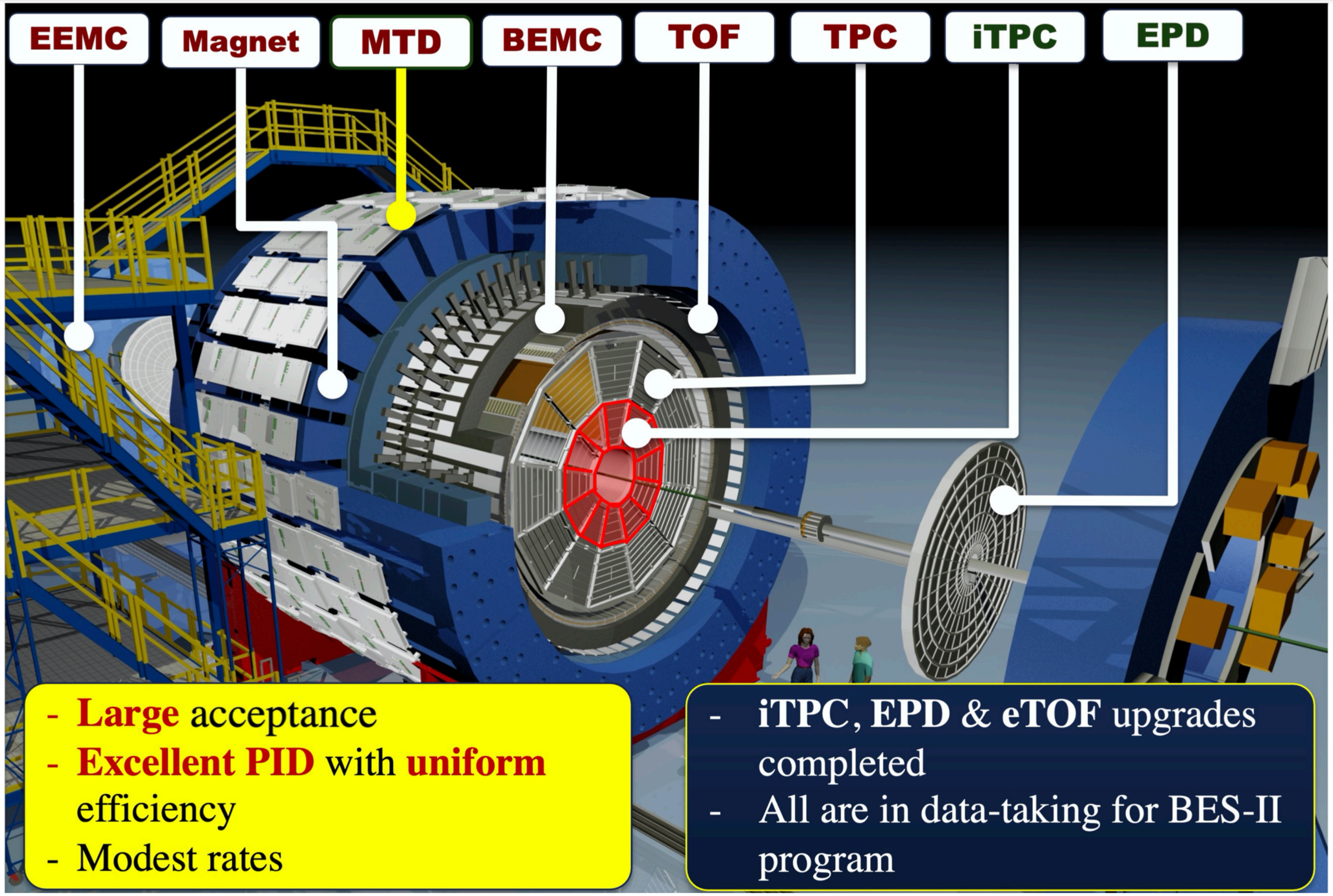

- **Large** acceptance
- **Excellent PID** with **uniform** efficiency
- Modest rates

- **iTPC**, **EPD** & **eTOF** upgrades completed
- All are in data-taking for BES-II program

1) Enlarged rapidity acceptance
2) Improved particle identification
3) Enhanced event plane resolution

- Major Upgrades in BES-II:

iTPC:
- Improves dE/dx
- Extends η coverage from 1.0 to 1.5
- Lowers p_T cut-in from 125 to 60 MeV/c
- Ready in 2019

eTOF:
- Forward rapidity coverage
- PID at η = -1.1 to -1.6
- Ready in 2019

EPD:
- Improves trigger
- Event plane measurements
- Ready in 2018

[1] iTPC: https://drupal.star.bnl.gov/STAR/starnotes/. public/sn0619.
[2] eTOF: STAR and CBM eTOF group, arXiv: 1609.05102.
[3] EPD: J. Adams, et al. NIM **A968,** 163970 (2020)

Dataset and Event Plane Reconstruction

DataSet	$\sqrt{s_{NN}}$ = 3.0 GeV (2018) (y_{target} = -1.04)	3.2 GeV (2019) (y_{target} = -1.14)	3.5 GeV (2020) (y_{target} = -1.25)	3.9 GeV (2020) (y_{target} = -1.37)	4.5 GeV (2020) (y_{target} = -1.52)
Events	~260 M	~210 M	~115 M	~120 M	~120 M

Event plane reconstruction

- EP reconstruction: Q vector method
- Re-center and shift calibration
- EP resolution: three sub-events method

The EP resolution is determined as:

$$R_1 = \langle \cos(\Psi_1^a - \Psi_r) \rangle$$

$$= \sqrt{\frac{\langle \cos(\Psi_1^a - \Psi_1^b) \rangle \langle \cos(\Psi_1^a - \Psi_1^c) \rangle}{\langle \cos(\Psi_1^b - \Psi_1^c) \rangle}}$$

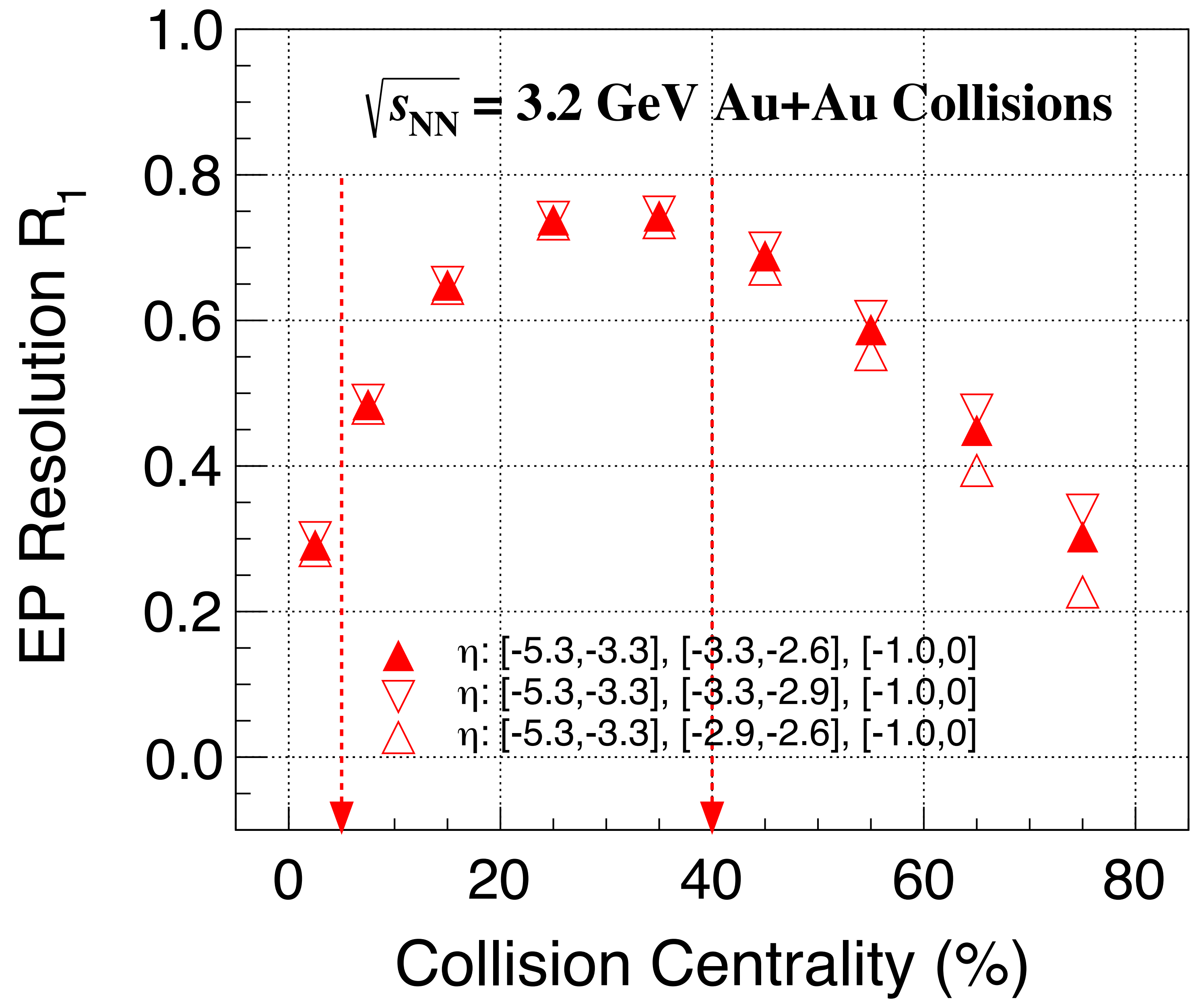

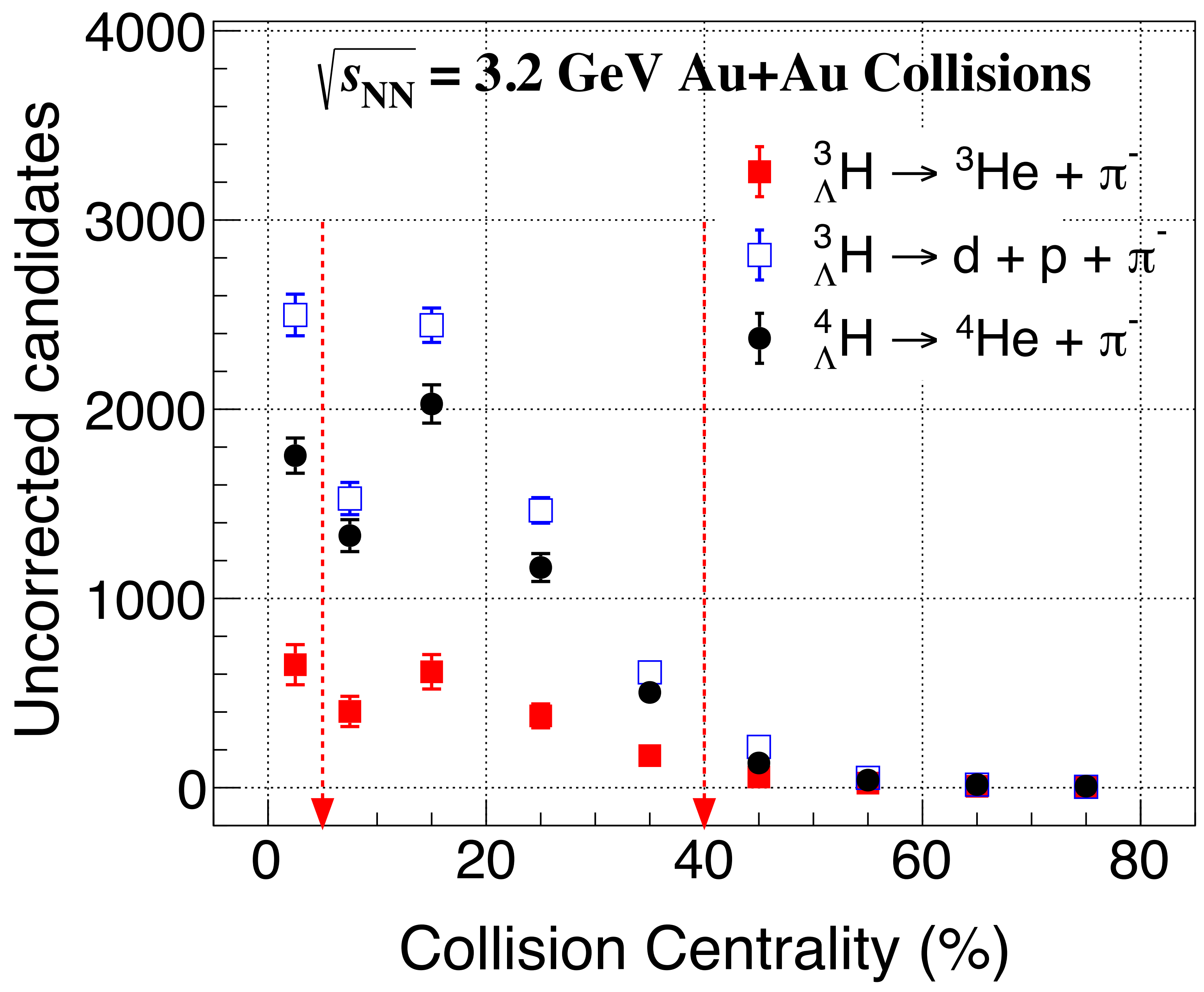

➢ 5-40% centrality bin used in this analysis

[1] A. M. Poskanzer and S. A. Voloshin, Phys. Rev. C **58,** 1671 (1998)

Particle Identification and Topological Selection

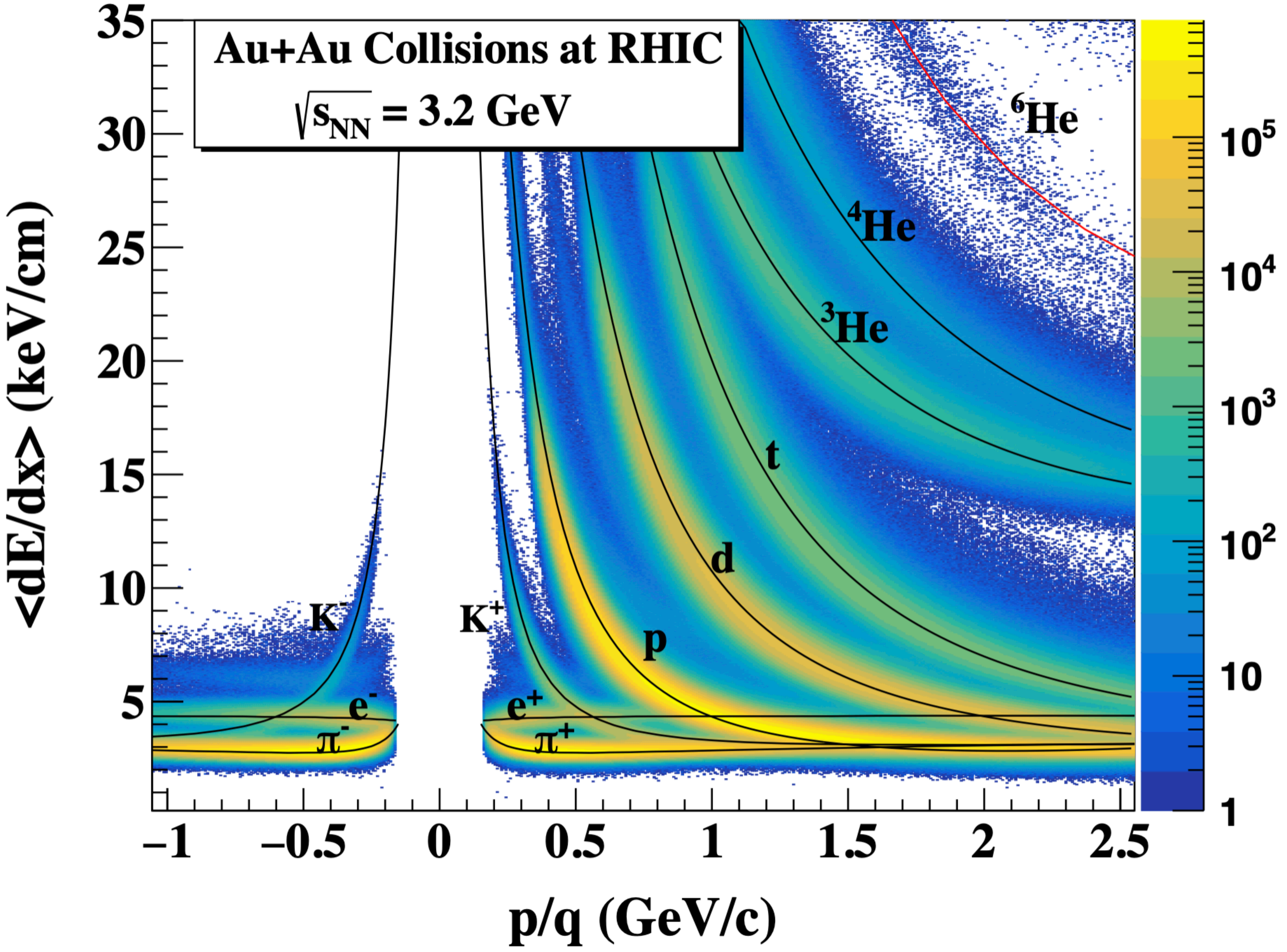

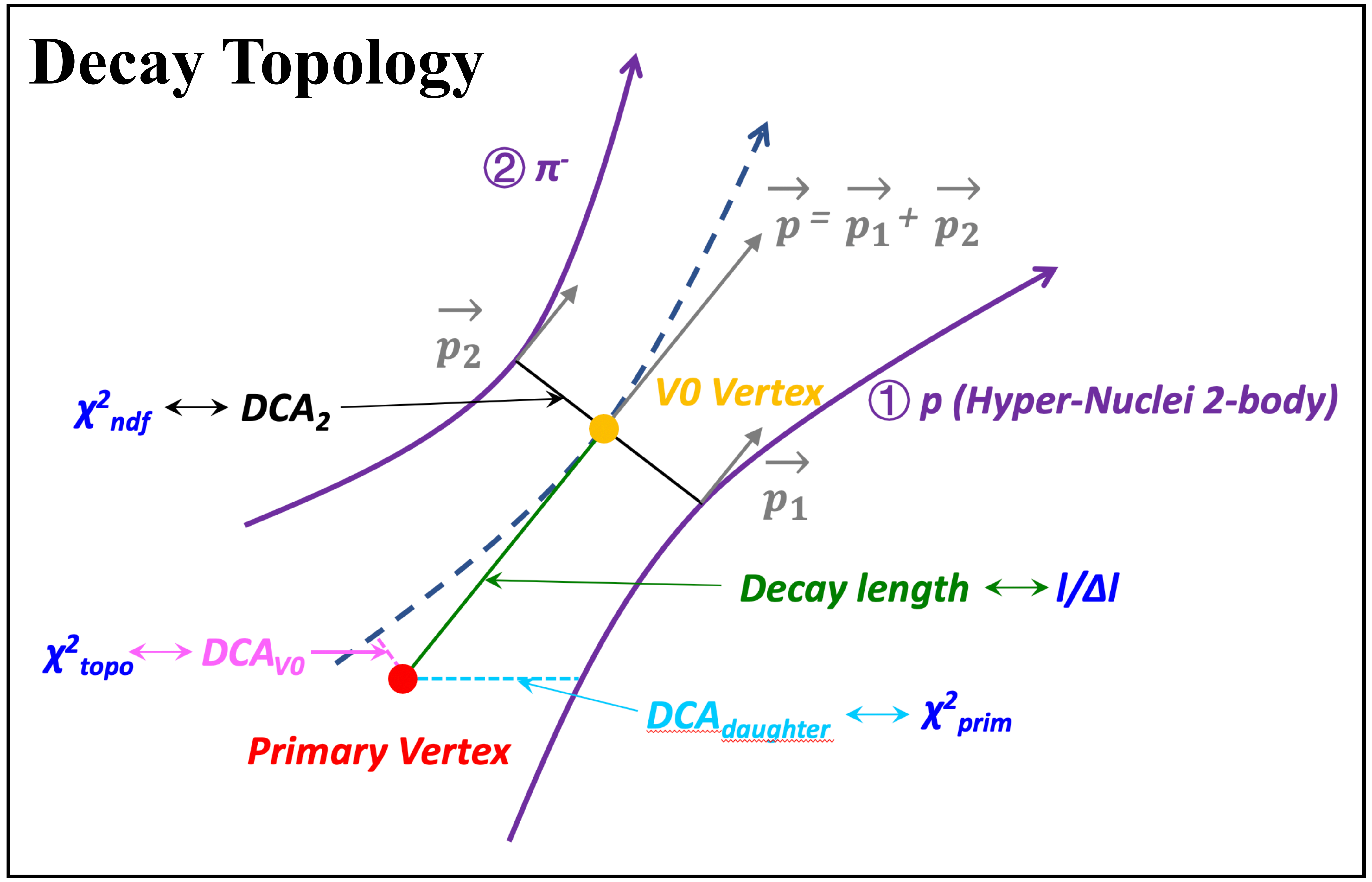

1) Good particle identification capability based on TPC and TOF
2) The hyper-nuclei reconstruction with KFParticle package based on the Kalman filter method providing a full set of the particle parameters together with their uncertainties
3) Decay topology tremendously helped on particle identification and background suppression

[1] Gorbunov and I. Kisel, Reconstruction of decayed particles based on the Kalman filter. CBM-SOFT-note-2007-003, 7 May 2007
[2] Ivan Kisel. Event Topology Reconstruction in the CBM Experiment. J. Phys. Conf. Ser. **1070(1)**, 012015 (2018)

Hyper-Nuclei Reconstruction

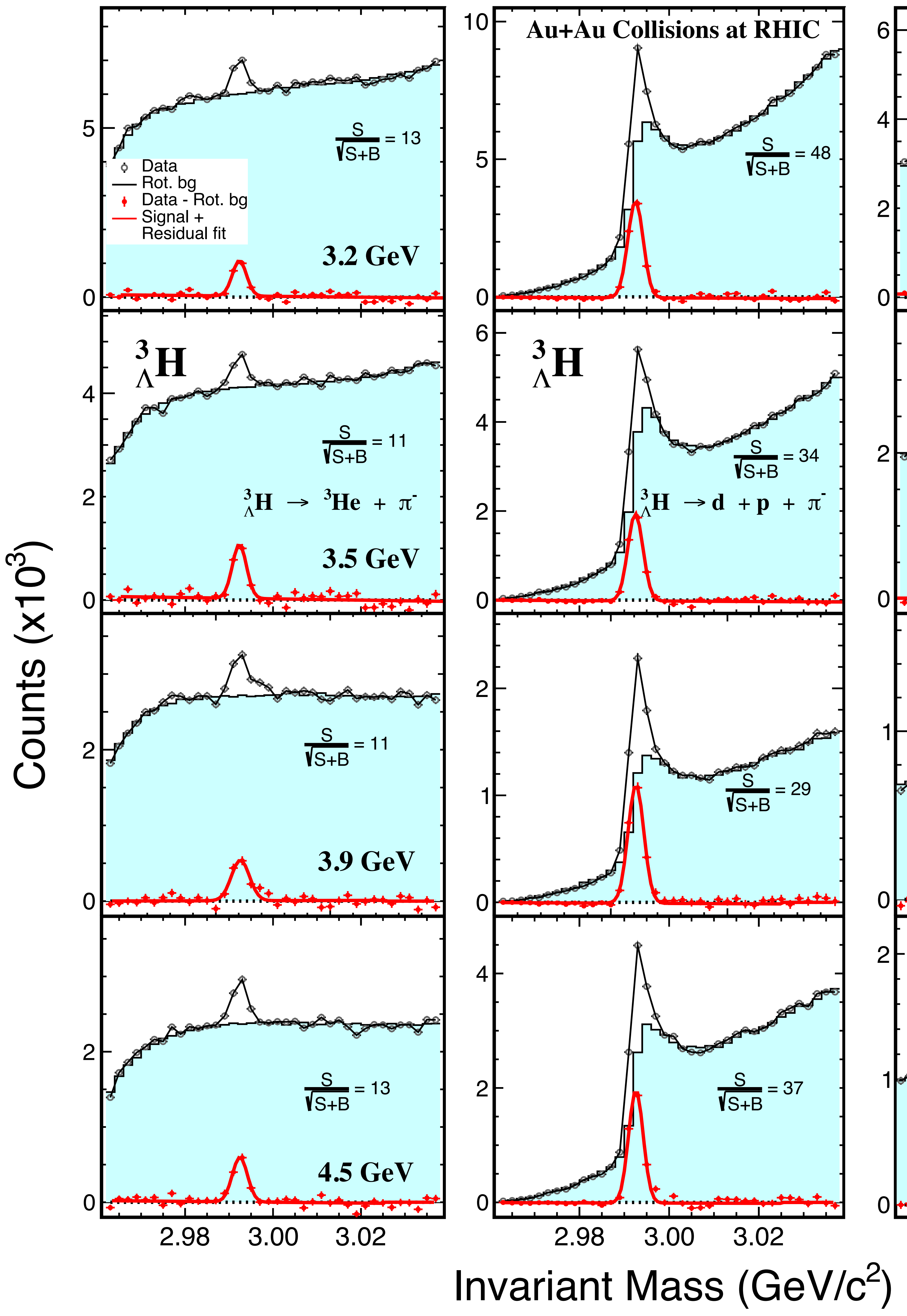

1) Topologically reconstructed $^{3}{}_{\Lambda}$H 2-body decay (left panel), 3-body decay (middle panel) and $^{4}{}_{\Lambda}$H (right panel) from 3.2, 3.5, 3.9 and 4.5 GeV Au+Au collisions

2) Background subtracted distributions are shown as red symbols. The significances of the mass peaks are also indicated

3) Obvious hyper-nuclei signals can be observed with the reconstructed invariant mass distributions

Acceptance of Λ, ${}^{3}_{\Lambda}$H and ${}^{4}_{\Lambda}$H of 3.2, 3.5, 3.9, 4.5 GeV

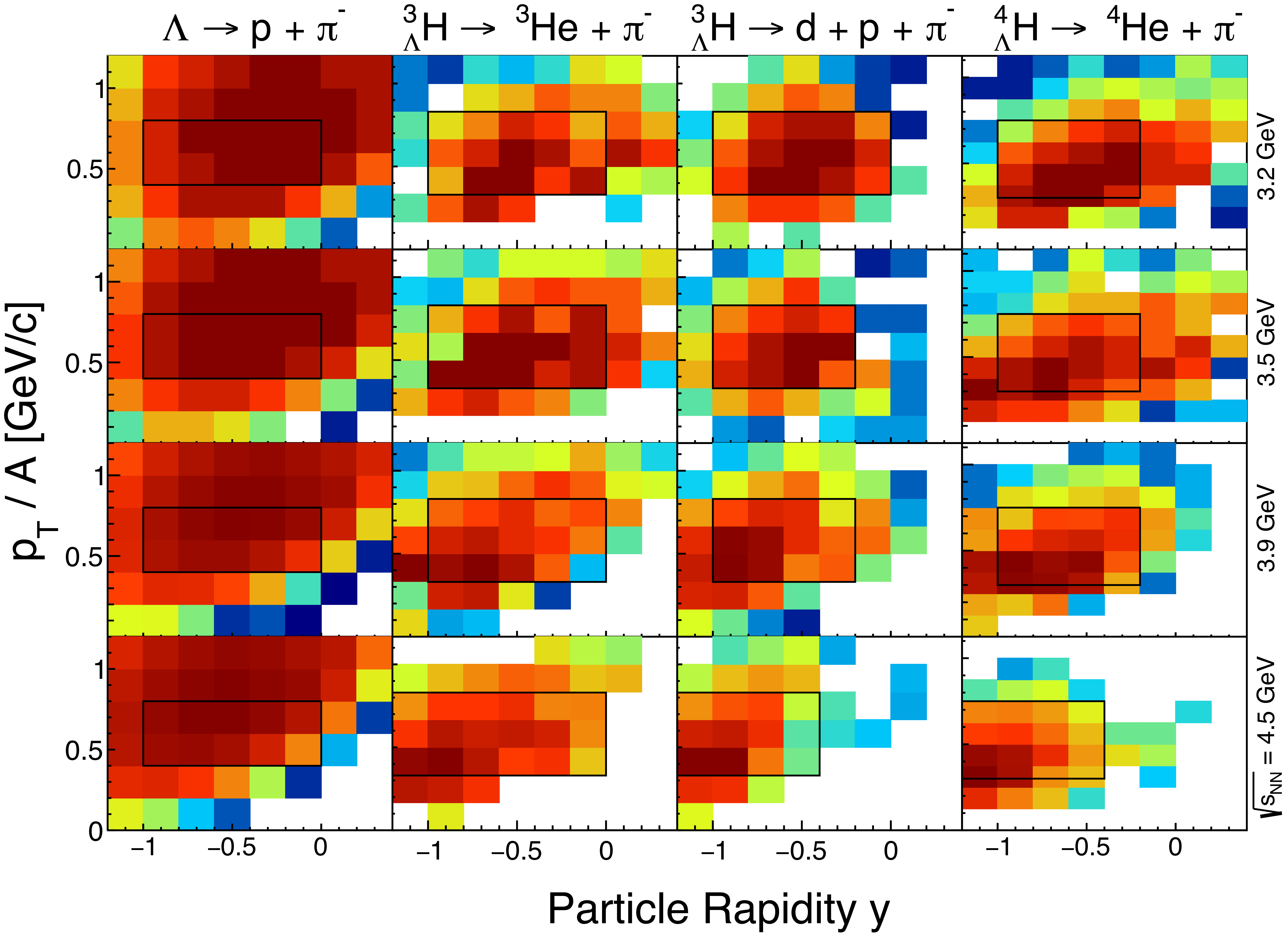

Directed flow of hyper-nuclei are calculated within the selected $0.4 \lesssim p_T / A \lesssim 0.8$ GeV/c range as indicated by the boxes

Acceptance of p, d, t, ^{3}He and ^{4}He of 3.2, 3.5, 3.9, 4.5 GeV

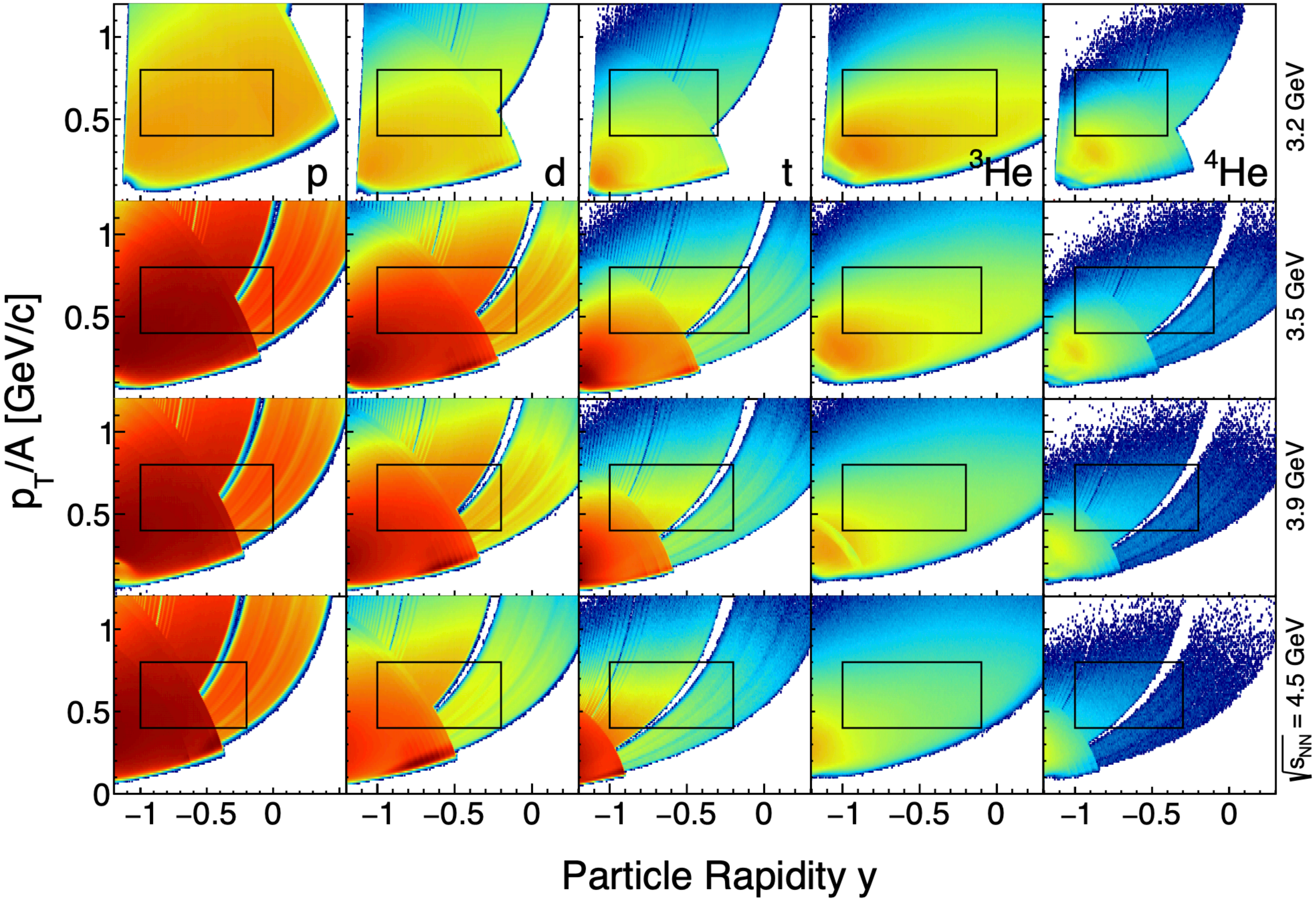

Directed flow of light-nuclei are calculated within the selected 0.4 < p_T / A< 0.8 GeV/c range as indicated by the boxes

Light- and Hyper-Nuclei Directed Flow v_1

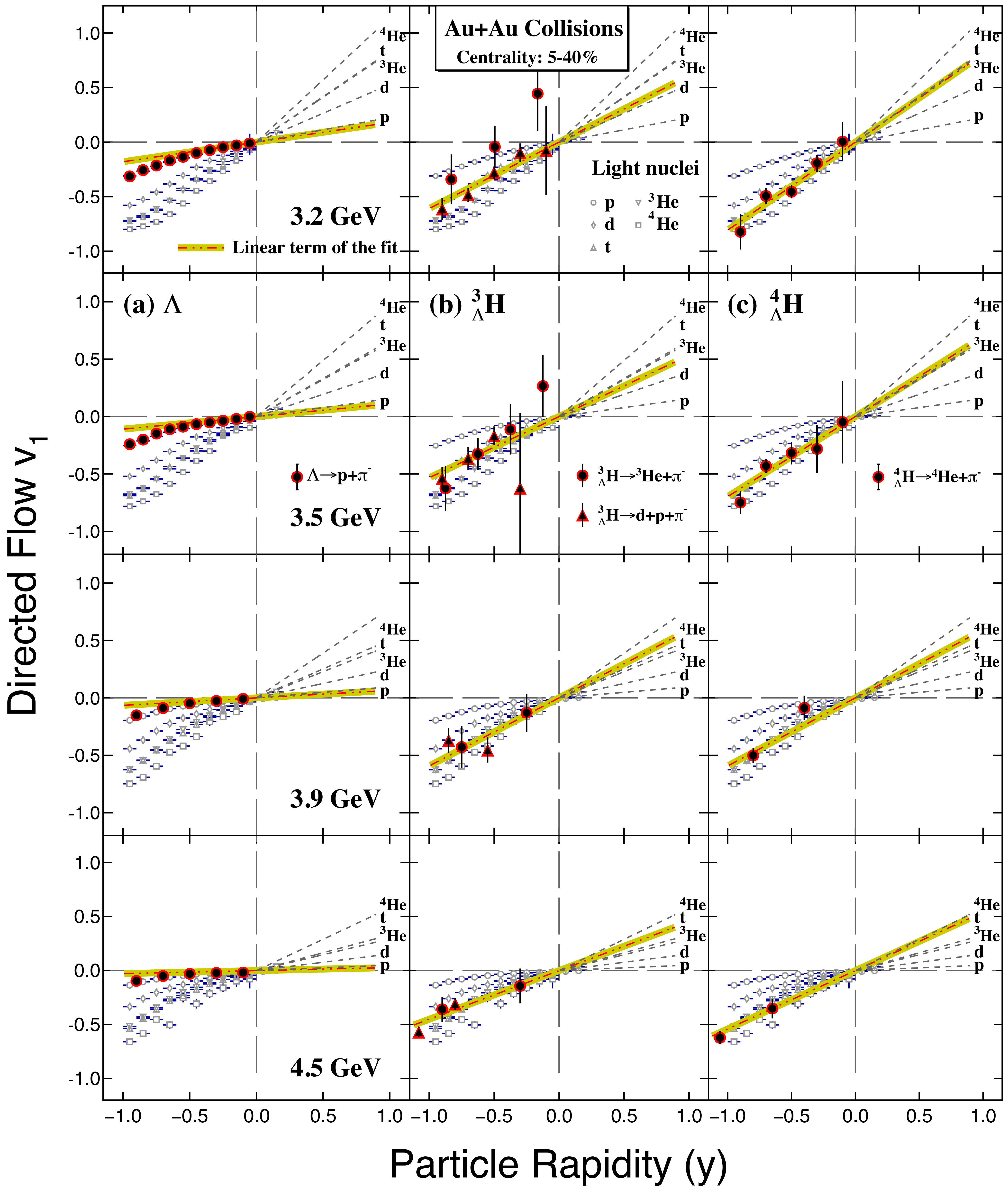

- The v_1 slope is obtained by fitting the $v_1(y)$ distribution with a polynomial function, where p_0 is the mid-rapidity slope $(v_1)^s = dv_1/dy\big|_{y=0}$

Hyper-Nuclei	Fitting Function	y	p_T / A
Λ	$v_1(y) = (v_1)^s \cdot y + p_1 \cdot y^3$	(-1.0, 0.0)	(0.4, 0.8)
$^3_\Lambda$H	$v_1(y) = (v_1)^s \cdot y$	(-1.0, 0.0)	(0.33, 0.83)
$^4_\Lambda$H	$v_1(y) = (v_1)^s \cdot y$	(-1.0, 0.0)	(0.30, 0.75)

Light-Nuclei	Fitting Function	y	p_T / A
p	$v_1(y) = (v_1)^s \cdot y + p_1 \cdot y^3$	(-1.0, 0.0)	(0.4, 0.8)
d	$v_1(y) = (v_1)^s \cdot y + p_1 \cdot y^3$	(-1.0, -0.2)	(0.4, 0.8)
t	$v_1(y) = (v_1)^s \cdot y + p_1 \cdot y^3$	(-1.0, -0.3)	(0.4, 0.8)
^{3}He	$v_1(y) = (v_1)^s \cdot y + p_1 \cdot y^3$	(-1.0, 0.0)	(0.4, 0.8)
^{4}He	$v_1(y) = (v_1)^s \cdot y + p_1 \cdot y^3$	(-1.0, -0.4)	(0.4, 0.8)

[1] M.S. Abdallah *et al*., (STAR Collaboration), Phys. Lett. B **827**, 136941 (2022)
[2] B. E. Aboona *et al*., (STAR Collaboration), Phys. Rev. Lett. **130**, 211301(2023)

Particle Mass Dependence

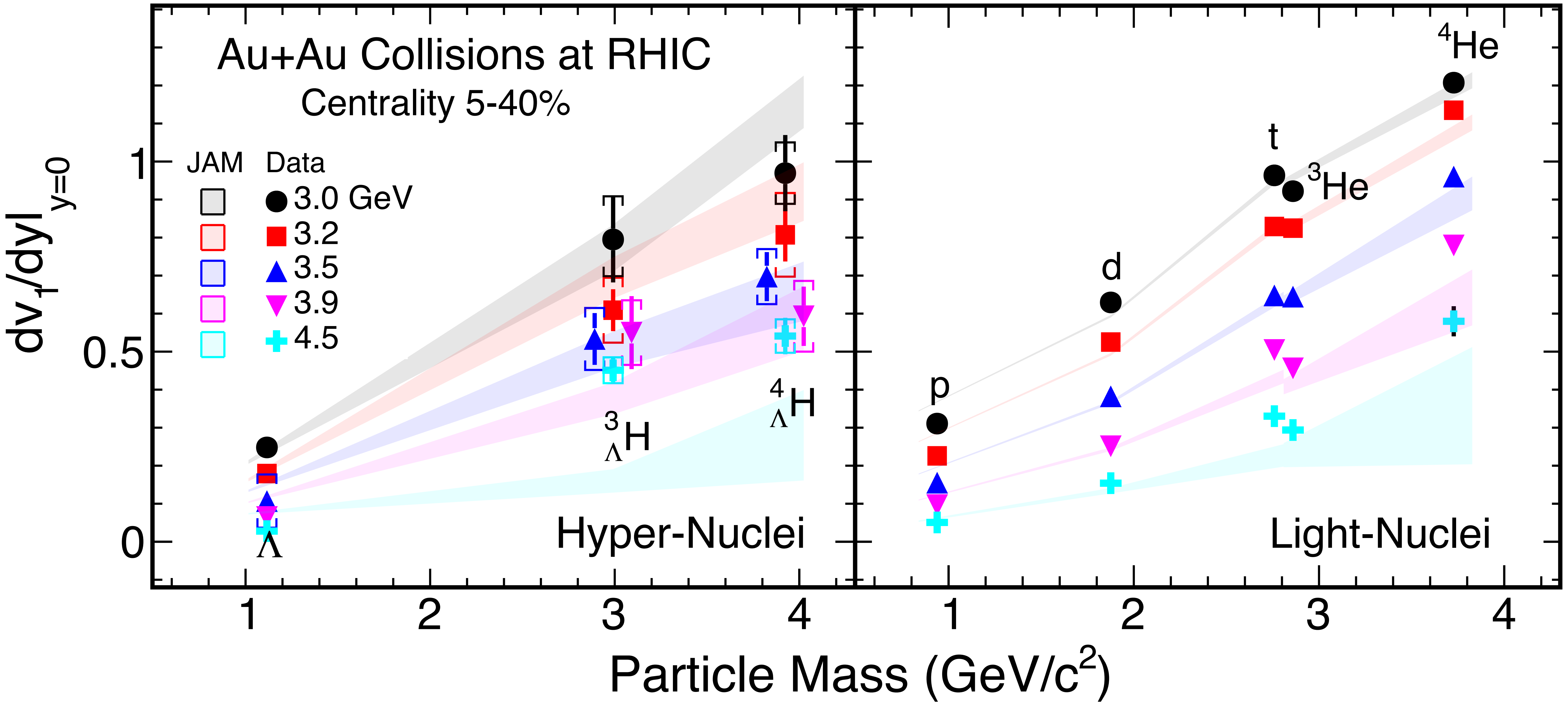

- Systematic uncertainties for v_1 slope:

Major source	$^{3}_{\Lambda}$H	$^{4}_{\Lambda}$H	light-nuclei
EP resolution	4%	4%	4%
Efficiency	2%	2%	2%
Topological cuts / PID cuts	12%	11%	5%
Total	13%	12%	6%

1) At given energy, for both light- and hyper-nuclei, it seems that the slopes of mid-rapidity v_1 are scaled with atomic mass number *A* or/and particle mass, implying coalescence is the dominant process for the light- and hyper-nuclei production
2) The feature is also reproduced by transport model JAM (mean field κ= 380 MeV) with coalescence afterburner calculations

Collision Energy Dependence

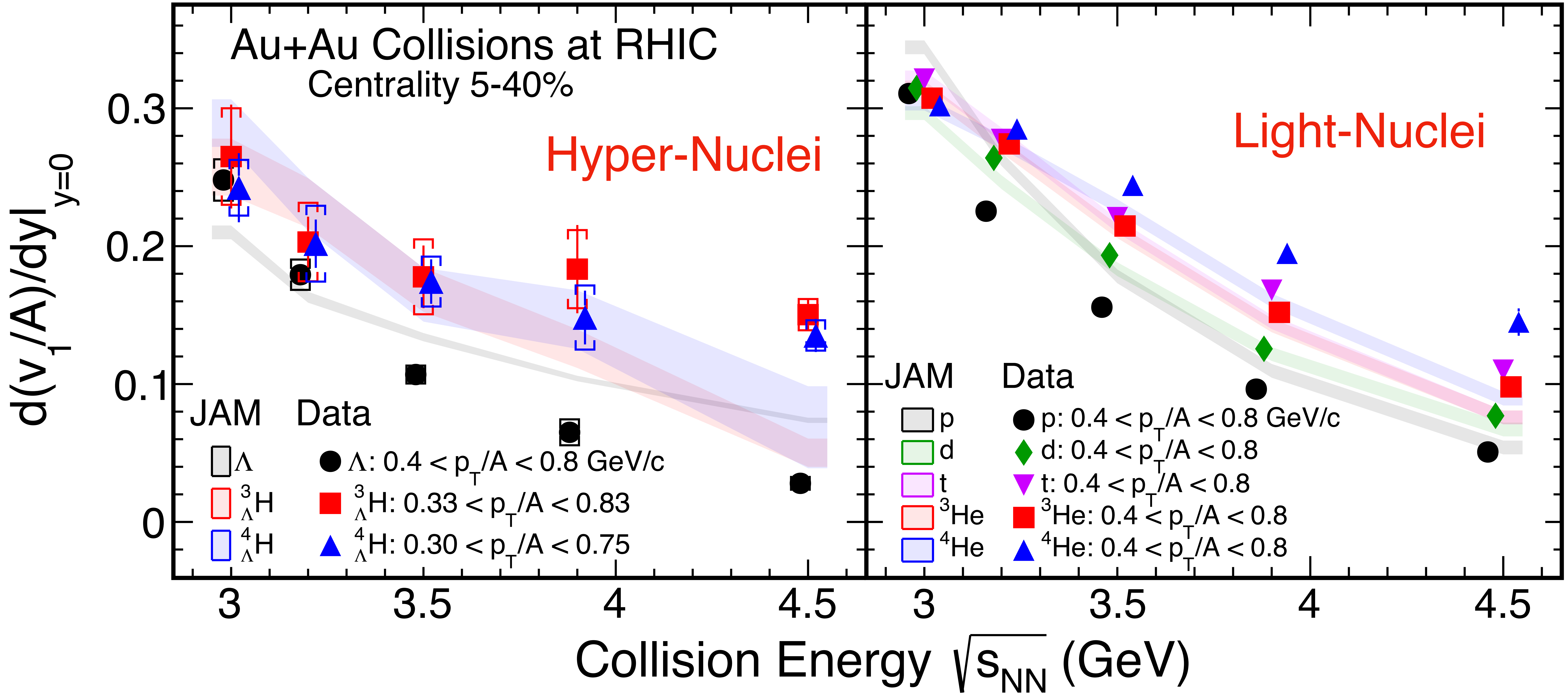

1) As the collision energy increases, the v_1 slope of light- and hyper-nuclei decreases

2) Hadronic transport model (JAM mean field κ= 380 MeV) plus coalescence afterburner calculations are consistent with observed energy dependence

Summary and Outlook

1) Studied the collision energy dependence of the directed flow v_1 for both light- and hyper-nuclei in $\sqrt{s_{NN}}$ = 3.0, 3.2, 3.5, 3.9, 4.5 GeV Au + Au collisions measured by the STAR experiment at RHIC

2) An approximate atomic mass number scaling and energy dependence are observed in the measured v_1 slopes of light- and hyper-nuclei at mid-rapidity

3) Calculations of hadronic transport model plus coalescence afterburner qualitatively reproduced the observed dependences for hyper-nuclei as well as light-nuclei implying coalescence process dominate the underlying production mechanism for those light clusters in these heavy ion collisions

Outlook:

2 billion events for 3.0 GeV Au + Au collisions at RHIC-STAR will significantly enhance the precision and help us to further constrain coalescence parameters for both light- and hyper-nuclei at the high density region

Thank you for your attention!